



Replacement of Conventional Base Course with Stabilized Lateritic Soil Using Ground Granulated Blast Furnace Slag and Alkali Solution in the Flexible Pavement Construction

S. Amulya¹ · A. U. Ravi Shankar¹

Received: 24 October 2019 / Accepted: 25 March 2020 / Published online: 13 April 2020
© Indian Geotechnical Society 2020

Abstract The use of cement/chemical-treated base and sub-bases is widely recommended in the pavement construction. Therefore, this paper investigates the behaviour of stabilized lateritic soil as a base course in flexible pavement by replacing the granular base course. The lateritic soil was stabilized with 25% Ground Granulated Blast Furnace Slag (GGBFS) along with the alkali solutions such as sodium hydroxide and sodium silicate at a varying sodium oxide (Na_2O) contents of 4, 5 and 6%, silica modulus (M_s , a ratio of silica to sodium oxide) of 0.5, 1.0 and 1.5 and a constant water binder ratio (w/b) of 0.25. The maximum compressive strengths of 5452 and 6593 kPa were achieved for a treated sample consisting of 6% Na_2O and 1.0 M_s cured for 28 days at the light and heavy compactions, respectively, which is due to the formation of calcium silicate hydrates when calcium oxide-rich GGBFS reacts with water. Further with the curing period results in an increase in strength due to the formation of calcium aluminosilicate hydrates when GGBFS reacts with alkali solutions. The durability of the samples was evaluated by wetting–drying and freezing–thawing tests. The samples passing the required durability criteria were tested for flexural strength and fatigue life. Scanning electron microscope images showed closely packed crystal orientation indicating high strength. Low and high volume pavements were designed using stabilized soil as a base course, and the strains were evaluated using pavement

analysis software. It is suggested that the conventional granular base layer can be replaced with the stabilized soil.

Keywords Lateritic soil · Fatigue · Microstructure · Stress–strain analysis · Pavement design · Chemical analysis

Introduction

Many infrastructure construction companies are facing problems in acquiring good materials due to the depletion of natural resources. In order to fulfill the demand of construction companies, locally available marginal materials blended with natural soil or aggregate can be used as an alternative material for construction [1, 2]. Lateritic soil is abundantly available which consists of quartz, feldspar, mica, hematite, goethite, gibbsite, kaolinite and oxides of silica, aluminium, iron and few traces of magnesium oxide, calcium oxide and sulfates [3–6]. Lateritic soil is formed due to tropical or subtropical weathering, and its chemical and morphological characteristics are influenced by the degree of weathering to which parent material is subjected [6]. As this soil is exposed to high temperature and humid, alternate wetting and drying, it shows poor engineering properties like low strength, high permeability, high moisture content and low density [7, 8]. In order to overcome the problematic effect of lateritic soil in road construction, the engineering properties of the soil have to be enhanced. The stabilization is a technique that alters the geotechnical properties [6, 9, 10]. The types of stabilizers are categorized based on the properties imparted during the stabilization of the soil such as stability, binding effect, waterproofing and retarders [11]. Many research works were carried out to stabilize the soil using quicklime

✉ S. Amulya
amulya2mail@gmail.com

A. U. Ravi Shankar
aurshankar@gmail.com

¹ National Institute of Technology Karnataka,
Surathkal, Mangalore, Karnataka 575025, India

[10, 12], areca nut coir fibre [13], bio-enzyme [14], Class F fly ash [15], sugar cane straw ash [16], geofibre and geogrid [17, 18], lime and geofibre or geotextile [19], ground granulated blast furnace slag (GGBFS) and cement [20]. The laboratory tests such as Unconfined Compressive Strength (UCS) and California Bearing Ratio (CBR) on soft soil stabilized with GGBFS were carried out and found 9% as optimum GGBFS content [21].

Apart from the addition of marginal materials, stabilization of soil can be done using the geopolymerization technique. The concept of geopolymerization involves the chemical reaction of aluminosilicate oxides with alkali polysilicates yielding polymeric Si–O–Al bonds [22]. The clay soil stabilized with the enzyme and alkali-activated GGBFS achieves the UCS 1.15 times better than ordinary Portland cement stabilized soil and 5.5 times better than enzyme stabilized soil at an optimum dosage of 20% GGBFS treated with 1 molar sodium hydroxide (NaOH) solution [23]. The clay soil stabilized with sodium silicate (Na_2SiO_3) showed an increase in UCS with increased M_s up to 2.5 and sodium oxide (Na_2O) content up to 8%, but further increase in M_s and Na_2O decreases the strength [19, 24, 25]. Similarly, potassium oxide (K_2O) at 8% helps in getting early strength and better results, but further increase in dosage to 10% will reduce the strength, which may be due to the usage of all K_2O particles to form calcium silicate hydrate (CSH) gel [26]. The fly ash-based geopolymer showed an increase in strength at the water binder ratio (w/b) of 0.25 to 0.35, and a further increase in w/b acts inversely proportional to the strength [27]. Also, the high compressive strength can be obtained when M_s was between 0.8 and 1.4 with 8% Na_2O at a higher curing temperature of 90 °C cured up to 72 h, but further increase in M_s to 2 decreases the strength [28]. The alkali-activated fly ash mortar consists of an alkaline modulus ratio of 1.23, Na_2O dosage of 150 kg/m³, and liquid to binder ratio of 0.5 was considered as an optimum mix [29, 30]. The combination of Na_2SiO_3 or potassium silicate and NaOH or potassium hydroxide is considered to be the best combination of alkali solutions to be used in alkali-activated geopolymers [31]. The best mix design of pumice-based geopolymer composites is obtained at 0.36 w/b ratio, 0.68 M_s and 10% Na_2O [32]. Microstructural studies were carried out on the soil stabilized with an enzyme [23], soil–cement [33], expansive black cotton soil by means of geopolymerization [34], alkali-activated olivine in soil stabilization [35] and soil stabilization using alkali-activated agro-waste reinforced with wollastonite fibre [36] and the crystal orientation of the samples were analyzed.

An attempt is made to use the geopolymerization technique into the stabilization of soil where the lateritic soil was treated with GGBFS and alkali solutions such as NaOH and Na_2SiO_3 . Based on the literature survey, 25% of

GGBFS and alkali solutions consisting of 4, 5 and 6% of Na_2O having M_s of 0.5, 1.0 and 1.5 at constant w/b of 0.25 were chosen. The objective of the work is to conduct the laboratory tests like light and heavy compaction to get optimum moisture content (OMC) and maximum dry unit weight (γ_d). The γ_d obtained from light compaction is used for low volume and heavy compaction for high volume pavements. The treated samples were air-cured at ambient temperature (25 °C) for 0 (immediately after casting), 3, 7 and 28 days and tested UCS, CBR, and durability [wetting–drying (WD) and freezing–thawing (FT)]. The durable samples were assessed for flexural strength and fatigue life. The microstructure images obtained from scanning electron microscope (SEM) technique were analyzed to know the crystal orientation of the durable samples and the design of high and low volume roads as suggested by using stabilized soil as a base course replacing conventional granular layer. The critical strains developed on the sub-grade and below the bituminous surface were analyzed using IITPAVE software.

Materials and Methodologies

In the present investigation, materials like lateritic soil, GGBFS, NaOH, Na_2SiO_3 and potable water were used. The lateritic soil is abundantly available in tropical and subtropical regions where rainfall is more than 3500 mm and was procured from Dakshina Kannada district, Karnataka, India. The geotechnical properties of the lateritic soil were tested in the laboratory and are tabulated in Table 1. GGBFS is a by-product of iron and steel industries procured from Jindal Steel Works (JSW) Hospet, Karnataka, India. The GGBFS is available in the form of a powder in a grey colour. The physical and chemical properties of the GGBFS are tabulated in Tables 2 and 3, respectively. The alkali materials such as NaOH and Na_2SiO_3 of industrial-grade were procured from Mangalore, Karnataka, India. The NaOH is in the form of flakes having a molecular weight of 40 g/mol with a specific gravity of 2.14 and Na_2SiO_3 in the form of liquid consisting of 18.7% of Na_2O , 32.5% of silica (SiO_2) and 48.8% of water having M_s 1.74. Na_2SiO_3 having a molecular weight of 285.1 g/mole and a specific gravity of 1.52.

Methodology

An oven-dried soil was used for all laboratory tests, and three trial samples were prepared for testing. The variance of all three trial values should be within the limits suggested by codes. The grain sieve analysis was done as per Indian Standards (IS): 1498–1970, and the lateritic soil is classified as highly compressible fine silty (MH) and

Table 1 The geotechnical properties of lateritic soil

Property	Value
Specific gravity	2.7
Grain size distribution	
(a) Gravel (%)	24
(b) Sand (%)	16
(c) Silt and clay (%)	60
Soil classification	CH
Atterberg limits	
(a) Liquid limit (%)	68
(b) Plastic limit (%)	30
(c) Plasticity index (%)	38
Light compaction	
(a) OMC (%)	25
(b) γ_d (kN/m ³)	15.7
Heavy compaction	
(a) OMC (%)	23
(b) γ_d (kN/m ³)	16.8
CBR	
Light compaction	
(a) Unsoaked condition (%)	8
(b) Soaked condition (%)	2
Heavy compaction	
(a) Unsoaked condition (%)	19
(b) Soaked condition (%)	8
UCS	
(a) Light compaction (kPa)	428
(b) Heavy compaction (kPa)	530

Table 2 Physical properties of GGBFS

Properties	Values
Specific gravity	2.78
Water content	24.5%
Size	<75 micron
Loss on ignition	0.05%

Table 3 Chemical properties of GGBFS

Chemical compounds	CaO	SiO ₂	Al ₂ O ₃	MgO
Quantity (%)	30–50	28–38	8–24	1–18

inorganic fat clays (CH) as per the Unified Soil Classification System (USCS). The specific gravity of soil and GGBFS were found as per, IS: 2720: Part 3: Sec 1: 1980. The Atterberg limits were found as per IS: 2720: Part 5:

1985 only for the natural soil with water. The soil treated with GGBFS and alkali solution becomes stiff; hence, Atterberg limits could not found. Both light and heavy compaction tests were carried out as per IS: 2720: Part 7: 1980 and IS: 2720: Part 8: 1983, respectively, for both untreated and treated soil. In India, the light compaction is adopted for the construction of low volume roads which carries traffic less than 1 million standard axles (msa) and heavy compaction is adopted for high volume roads. The UCS test was conducted as per IS: 2720: Part 10: 1991 on cylindrical samples having 38 mm diameter and 76 mm height for both light and heavy compaction. The prepared samples were air-cured at an average ambient temperature of 27 °C for different curing periods of 0 (immediately after mixing), 3, 7 and 28 days, and the gradual axial load is applied at the rate of 1.25 mm/s. The cylindrical CBR molds were prepared for both light and heavy compaction and cured for different curing periods. The prepared samples were tested at both soaked and unsoaked conditions as per IS: 2720-16 1987 at a gradual application of load at the rate of 1.25 mm/s. The durability tests include WD and FT and were conducted on UCS samples. The WD test is conducted as per ASTM 559 D by immersing the samples in water for 5 h and oven-dried for 42 h at 71 °C. Each wetting and drying process constitutes one cycle. The weight loss of samples at the end of each cycle is measured. The percentage weight loss after 12 cycles of wetting and drying should not exceed 14%. Similarly, the FT test was conducted as per ASTM 560 D where the cured samples were kept at – 23 °C for 24 h and thaw at 21 °C for 23 h which constitutes one cycle. Percentage weight loss after 12 cycles was calculated, and it should not exceed 14%. The rectangular beam samples 300 × 75 × 75 mm dimension were cast for both light and heavy compaction and cured for 28 days. The test was conducted as per IS: 4332: Part 6: 1972 by applying the gradual load of 1.25 mm/s longitudinally under a two-point loading condition. The load at which the crack occurs on the sample is used for the calculation of the flexural strength of the stabilized soil. The fatigue test was conducted on the UCS samples cured for 28 days under repeated application of the load and the number of repetitions at which sample fails were noted down. The chemical composition of the stabilized soil includes determining the quantity of oxides such as SiO₂, Fe₂O₃, Al₂O₃, CaO and MgO. SiO₂, Fe₂O₃ and Al₂O₃ were found as per IS: 2720: Part 25: 1982, and the quantity of CaO and MgO was found from titration. The design of low volume and high volume roads was done using Indian Roads Congress (IRC): SP: 72-2015 and IRC: 37-2018, respectively.

Results and Discussion

Compaction Tests

The OMC and γ_d of the stabilized soil obtained from light and heavy compaction are depicted in Fig. 1a, b. The light and heavy compactions are represented as L and H, respectively. The samples are represented in x - y - z form, where x is the % of GGBFS (25%), y is % of Na_2O (4, 5 and 6%) and z is the M_s (0.5, 1.0 and 1.5). For example, 25-4-0.5 indicates 25% GGBFS, 4% Na_2O and 0.5 M_s .

The γ_d of 16.8 and 18.05 kN/m^3 was achieved for the treated soil sample of 25-6-1.0 for light and heavy compaction, respectively. Due to the compaction effort, the voids will be squeezed and filled with fines and hence, the density was achieved [13, 37]. It was observed that the OMC increases with an increase in M_s which may be due to the increased Na_2SiO_3 which increases the water content and hence, γ_d decreases [27].

Unconfined Compressive Strength (UCS) Test

The treated soil samples were air-cured for 0, 3, 7 and 28 days and tested. The variation in compressive strength of the samples at different curing periods is depicted in Fig. 2a–c.

Effect of Curing Period on UCS

From Fig. 2a–d, it is inferred that as the curing period increases from 0 to 28 days, the UCS increases. The treated lateritic soil sample of 25-6-1.0 has achieved the maximum UCS of 5452 and 6593 kPa after 28 days of curing which is 11.7 and 11.4 times more than that of the natural soil for the light and heavy compaction, respectively. It is observed that when the curing period increases from 0 to 7 days, there is a rapid increase in UCS. The exothermic reaction between GGBFS and alkali solution generates heat which

increases the rate of polymerization and forms the calcium silicate hydrates (CSH) bond to achieve the initial strength [38]. Further increase in the curing period to 28 days helps in the gradual polymerization reaction and forms the calcium alumino-silicate hydrates (CASH or alumino-silicate structure) [38].

Effect of Na_2O Dosage on UCS

As the Na_2O dosage increases from 4 to 6%, the UCS increases due to the increased rate of polymerization and hence, high compressive strength is achieved which is evident from Fig. 2a–d. The higher Na_2O dosage of 6% creates the aqueous environment and helps in the dissolution process of polymerization, due to which the cohesiveness and fluidity in the mix increase and hence, the bonding of particles increases [39, 40].

Effect of M_s on UCS

As M_s increases from 0.5 to 1.0, the UCS increases rapidly and a further increase in M_s to 1.5 decreases the UCS for both light and heavy compactions. Increase in UCS at 1.0 M_s is due to the equal concentration of SiO_2 and Na_2O content helps to strengthen the sample due to stable alumino-silicate structure. Further increase of M_s to 1.5 decreases the UCS due to increased Na_2SiO_3 which precipitates extra SiO_2 content on the surface of the sample causes detrimental effects such as efflorescence and brittleness [24, 41]. Also, Na_2SiO_3 concentration increases the water content in the mix and hence, the strength decreases [27].

California Bearing Ratio Test

The CBR test at soaked and unsoaked conditions was conducted on the treated samples for both light and heavy compactions. It was observed that the treated soil becomes

Fig. 1 The variation in OMC and γ_d of stabilized soil obtained from light and heavy compaction

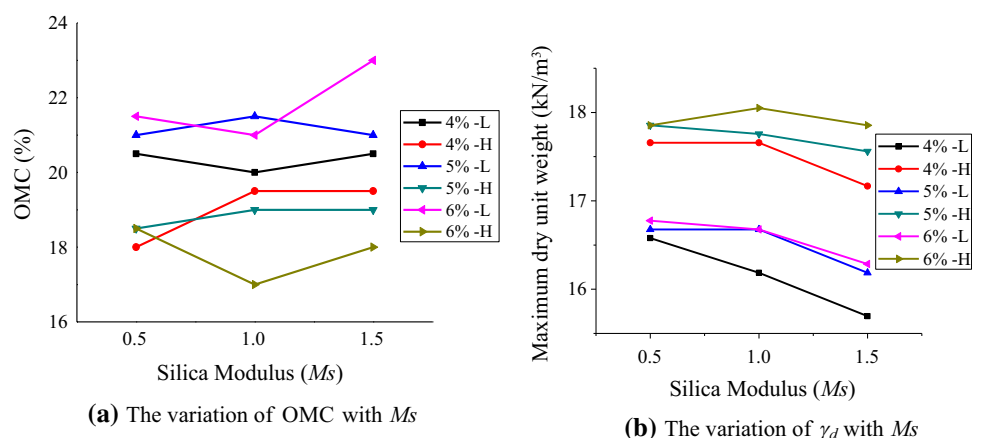
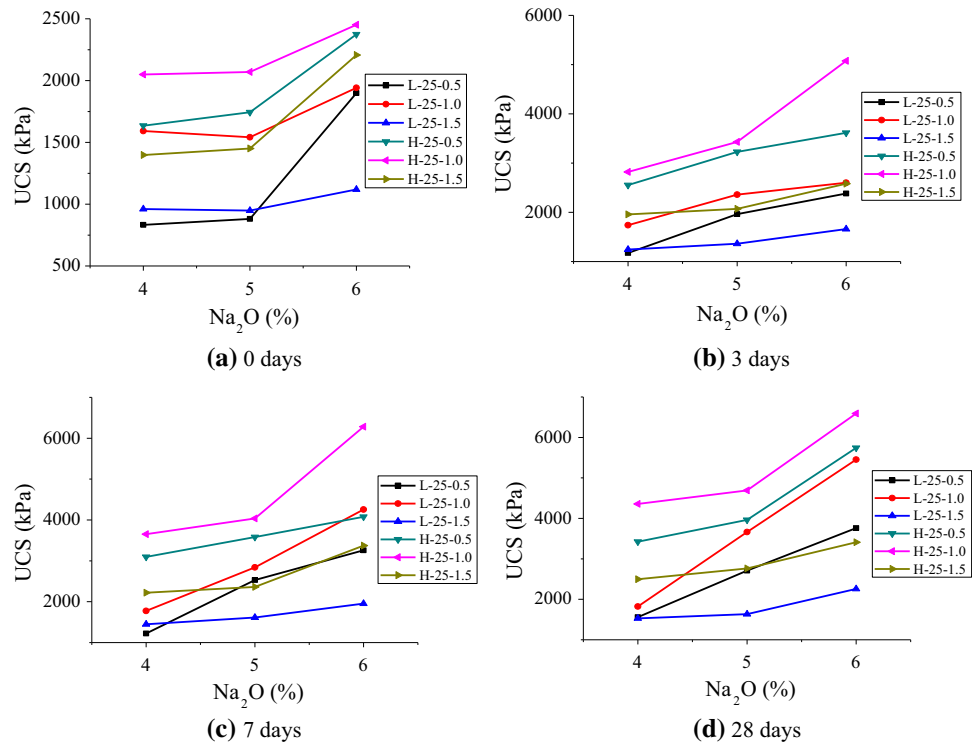


Fig. 2 The variation in UCS for different curing periods



stiff and impermeable. The moisture absorption after 4 days soaking is found only 15% and due to which the plunger could not penetrate into the sample. Due to this, the penetration resistance values were very high and CBR values were found to be more than 100% which is unrealistic. Therefore, in order to ensure the strength of the stabilized soil as a base course material, the durability test was conducted.

Effect of Durability Test

The durability of the road materials should maintain stability, integrity and bonding with the soil under cyclic weathering change and adverse conditions over years of exposure [42]. In the present work, the durability test was conducted on stabilized samples air-cured for 0, 3, 7 and 28 days for light and heavy compactions and the results are tabulated in Table 4 and sample images are shown in Fig. 3a–c.

From Table 4, it is evident that the treated sample of 25-5-1.0 passed the durability after 28 days curing and treated a sample of 25-6-0.5 passed durability after 7- and 28-days curing for light and heavy compactions. Similarly, the treated sample of 25-6-1.0 passed the durability after 3, 7- and 28-days curing. It is observed that as there is an increase in the dosage of Na₂O till 6% and *M_s* till 1.0, the UCS increases which are due to the formation of aluminosilicate structure [37]. Therefore, hereafter the samples of 25-5-1.0, 25-6-0.5 and 25-6-1.0 for both light and heavy

compactions cured for 28 days are considered for flexural, fatigue tests and microstructure analysis.

Flexural Strength Test

The rectangular beam was cast for durable samples and cured for 28 days for both compactions. The samples were tested under two-point loading, and the gradual load was applied. The loads at which the crack occurs were noted down, and the resilient modulus of the samples is calculated using Eq. (1) suggested by IS: 4332: Part 6: 1972 where the weight of the beam is neglected.

$$M_R = \frac{Pl}{bd^2} \tag{1}$$

where *P*—maximum applied load in kN, *l*—span length in mm, *b*—average width of the specimen in mm, *d*—average depth of the specimen in mm, *M_R*—Modulus of rupture in MPa.

The flexural strength test results are depicted in Fig. 4.

From Fig. 4, it is observed that the treated sample of 25-6-0.5 is showing the highest flexural strength of 0.62 and 0.63 MPa for light and heavy compactions, respectively. The flexural failure (crack) occurred at the center of the sample, and the failed specimen is shown in Fig. 5.

Table 4 Percentage weight loss of stabilized samples after 12 cycles of durability test

Particulars	Percentage weight loss after 12 cycles of durability test							
	Curing period (days)							
	0		3		7		28	
	WD	FT	WD	FT	WD	FT	WD	FT
Light compaction								
L-25-4-0.5	1st	13.2	1st	8.2	1st	8	1st	2.6
L-25-4-1.0	1st	12.5	1st	8.1	1st	7.9	1st	2.1
L-25-4-1.5	1st	12.1	1st	8.7	1st	6.1	1st	1.8
L-25-5-0.5	1st	11.9	1st	6.8	6th	4.3	9th	0.5
L-25-5-1.0	1st	12.8	4th	7.8	8th	1.2	5.3	0.4
L-25-5-1.5	1st	14	1st	7.2	1st	0.3	1st	0.1
L-25-6-0.5	1st	11.9	1st	5.2	5.1	0.5	6.9	0.9
L-25-6-1.0	1st	11.6	10.9	6.1	6.2	0.5	5.4	1
L-25-6-1.5	1st	5.8	1st	5	4th	2.6	5th	3.3
Heavy compaction								
H-25-4-0.5	1st	13.2	1st	8.0	1st	5.8	1st	1.8
H-25-4-1.0	1st	13.6	1st	9.3	1st	8.6	1st	3.5
H-25-4-1.5	1st	13.6	1st	9.3	1st	8.6	1st	3.5
H-25-5-0.5	1st	10.6	1st	3.4	5th	3.2	5th	0.1
H-25-5-1.0	1st	13.1	6th	6.3	7th	3.1	8.4	1.3
H-25-5-1.5	1st	12.9	1st	7.6	1st	1.7	8th	2.3
H-25-6-0.5	1st	9.6	5th	4.8	7.9	2.4	9.6	1.5
H-25-6-1.0	1st	9.7	2.6	2.1	8.6	0.6	5.8	0.8
H-25-6-1.5	1st	1.6	1st	1.2	1st	2.7	4th	1.3

Numbers in the table represent the percentage weight loss, and the number with superscript represents the number of cycles

Fatigue Test

The fatigue test is carried out to find the fatigue life of treated samples under repeated application of load. The least UCS of 4232 and 5427 kPa that was achieved by the sample of 25-5-1.0 for the light and heavy compaction, respectively, was considered. The least UCS values were considered as it is genuine to compare the results with other durable samples which are having different combinations. The 1/3rd (0.33), 1/2 (0.5) and 2/3rd (0.66) of the UCS load were applied at a frequency of 1 Hz, and the variation in fatigue life is depicted in Fig. 6. The fatigue test set up is shown in Fig. 7.

The sample of 25-6-1.0 is sustaining maximum repetitions of 5.1×10^5 and 5.5×10^5 for the light and heavy compactions, respectively. The obtained fatigue life may be due to the achieved high strength and density.

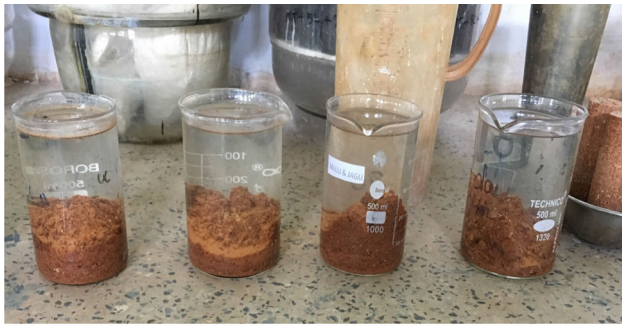
Microstructure Analysis

The treated samples cured for 28 days are scanned under a high beam electron to obtain the microstructure images

using scanning electron microscope (SEM) technique with different resolutions. For the present work, the samples having $\times 2000$ resolution and 10 microns were compared. The samples prepared for light compaction and heavy compaction are depicted in Figs. 8a–c and 9a–c, respectively.

From Fig. 8a–c, it is observed that the grey coloured flake-like structure shows the microstructure image of GGBFS reacted with alkali solutions and the black spot represents the void formation due to the unreacted GGBFS and alkali solution. The treated samples consisting of 5% Na₂O dosage are showing more voids than that of the samples consisting of 6% Na₂O. Among all samples, the samples with a high dosage of Na₂O and *M_s* are giving a compact and closely packed structure which helps to achieve more strength.

Comparing microstructure images of treated samples obtained from heavy compaction shown in Fig. 9a–c, the compact and closely packed structure is achieved at high Na₂O (6%) dosage and *M_s* (1.0). It is also observed that the samples with *M_s* 0.5 are showing many voids than that of *M_s* 1.0. Due to the high density obtained from compaction,



(a) Samples collapsed during the WD test.



(b) Samples were taken out from freezer during FT test.



(c) Durability sustained sample after 12 cycles of the WD test.

Fig. 3 Durability tested samples

the samples prepared by heavy compaction are showing more interlocking of particles than the samples prepared by light compaction [35, 36].

Chemical Analysis

The chemical composition of the stabilized samples such as SiO₂, Fe₂O₃ and Al₂O₃ was found as per IS: 2720 (Part 25) —1982, whereas CaO and MgO were found by titration. The oxides of silica and alumina help the polymerization process to form an aluminosilicate (Si–O–Al) structure in the stabilized soil. It is noticed that samples prepared for heavy compaction are utilizing more silica and aluminates than the treated sample prepared by light compaction and

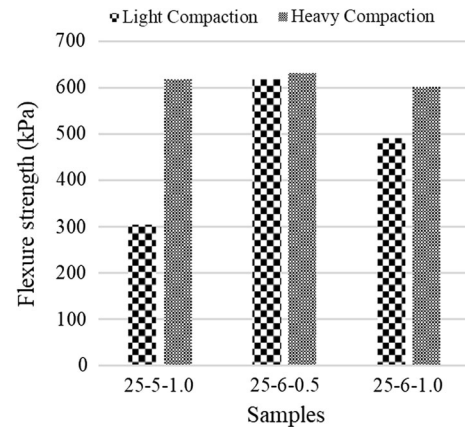


Fig. 4 Variation in flexural strength of the durability passed stabilized soil



Fig. 5 Failed sample during the flexure test

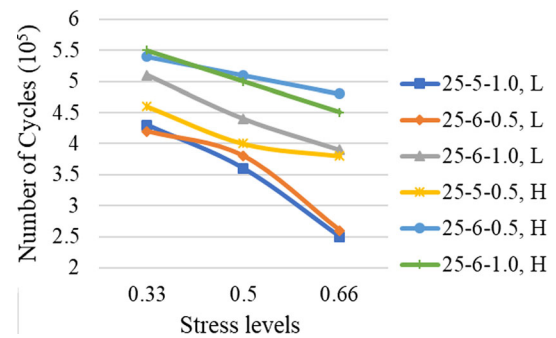


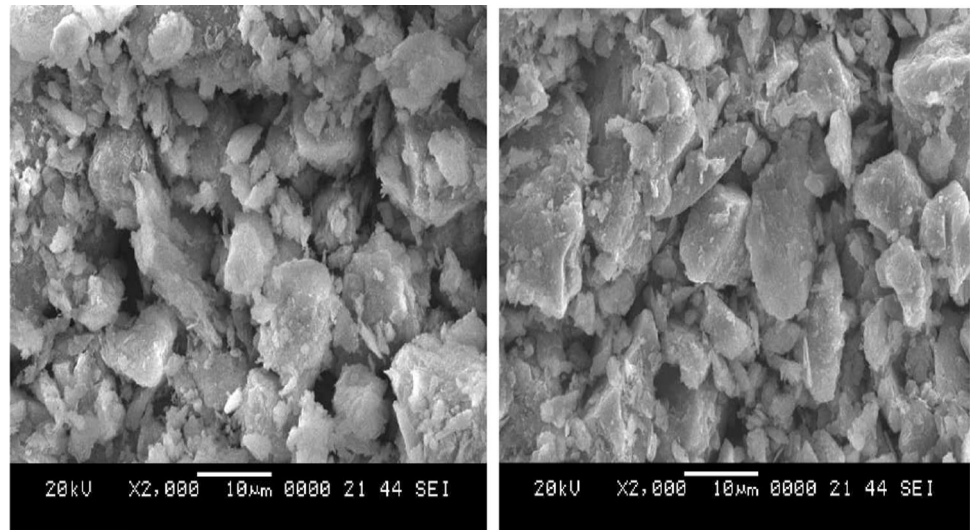
Fig. 6 Variation of the number of cycles for stabilized soil under repetitive loading conditions

due to which the strength and density have achieved. As Na₂O and Ms increases, the pH of the mixture increases [41]. Hence, the alkalinity in the mixture helps in achieving better bonding, strength and the results are tabulated in Table 5.

Fig. 7 Fatigue test setup

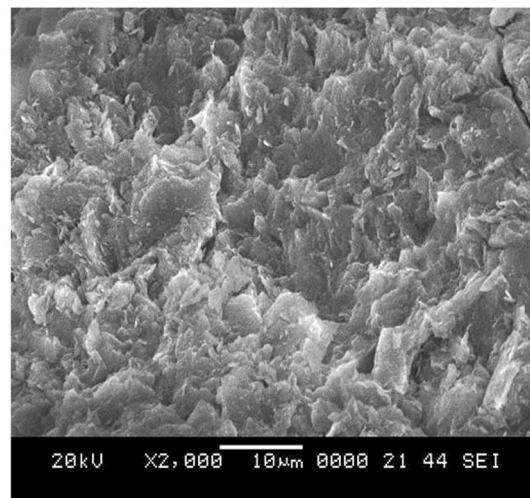


Fig. 8 The microstructure images of the durable samples for light compaction



(a) 25-5-1.0

(b) 25-6-0.5



(c) 25-6-1.0

Fig. 9 Microstructure images of durable samples for heavy compaction

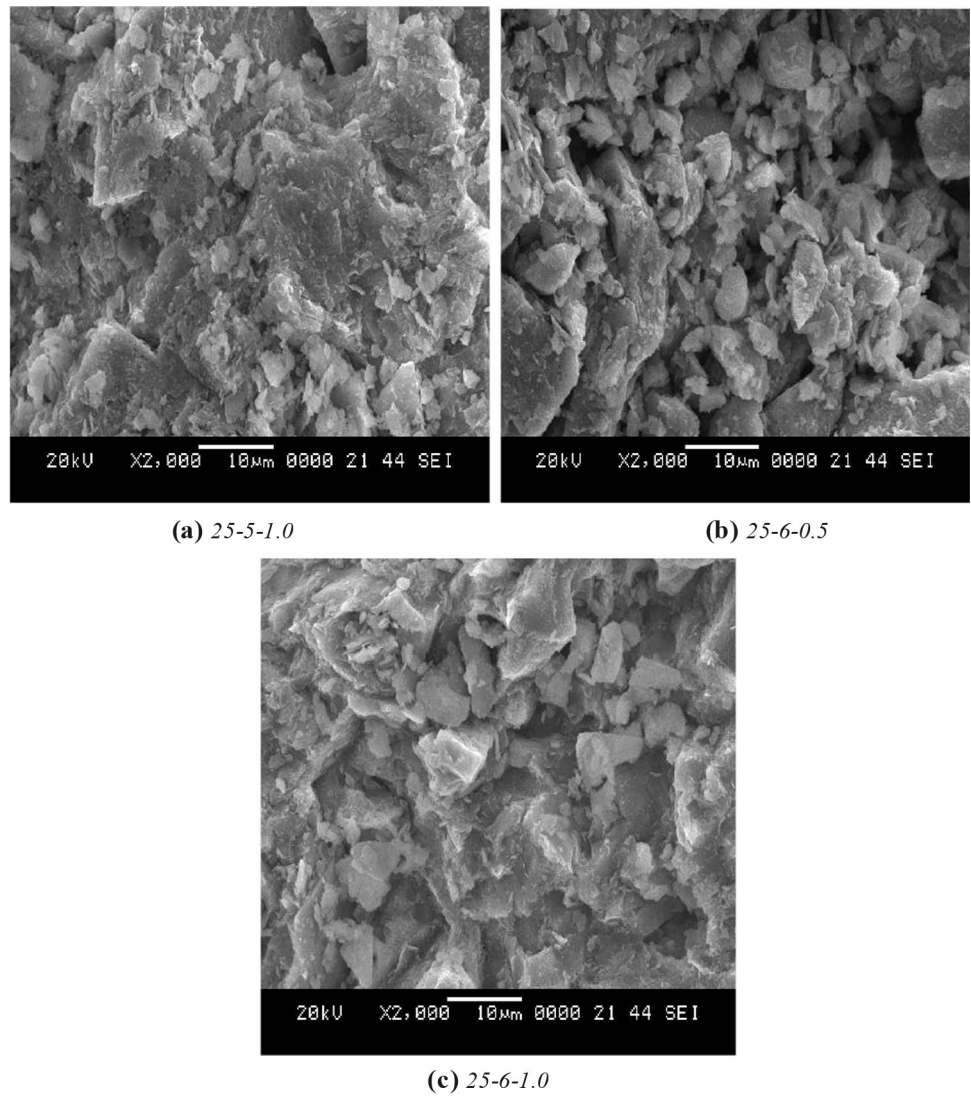


Table 5 The chemical composition of durability passed stabilized samples cured for 28 days

Samples	Compaction	Oxides (%)					pH
		SiO ₂	Fe ₂ O ₃	Al ₂ O ₃	CaO	MgO	
Natural soil		69.7	5.3	10.0	0.1	0.005	5.01
25-5-1.0	Light	52.5	3.7	11.7	0.2	0.04	10.39
25-6-0.5		50.7	3.1	10.0	0.18	0.04	10.42
25-6-1.0		51.6	4.0	8.4	0.18	0.02	10.54
25-5-1.0	Heavy	41.7	3.9	7.6	0.13	0.005	10.38
25-6-0.5		43.2	3.8	6.8	0.14	0.03	10.44
25-6-1.0		43.3	3.99	5.7	0.15	0.05	10.51

Table 6 The design of low volume conventional flexible pavement

Traffic ($\times 10^3$)	Thickness (mm) of convention				
	Modified soil	Gravel base	WBM Grade-3	Granular subbase	Base of gravel
10–30	100	200	–	–	–
30–60	100	150	75	–	–
60–100	100	–	75	125	75
100–200	150	–	75	125	75
200–300	150	–	75	175	75
300–600	150	–	75	250	75
600–1000	225	–	75	200	150
1000–1500	200	–	75	225	150
1500–2000	200	–	–	250	225

Table 7 The design of flexible pavements using stabilized soil

Traffic ($\times 10^3$)	Thickness (mm)			
	Cement-treated subbase, stabilized soil of 25-6-1.0	Cement-treated base, stabilized soil of 25-6-1.0	Crack relief aggregate layer	Bituminous macadam
10–30	100	150	–	–
30–60	110	150	–	–
60–100	120	150	–	–
100–200	125	150	–	–
200–300	130	150	–	–
300–600	125	150	75	–
600–1000	100	150	125	–
1000–1500	125	150	125	–
1500–2000	125	150	75	50

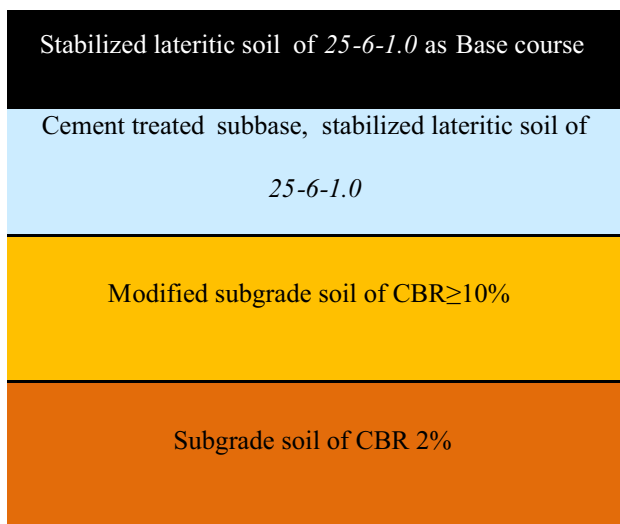


Fig. 10 The cross section of the flexible pavement using stabilized soil

Application of Stabilized Soil in Flexible Pavement Construction

Low Volume Roads

The low volume pavement design is suggested as per Indian Roads Congress (IRC): SP:72-2015, and the pavement thickness for low volume roads is tabulated in Table 6. The soaked CBR of the subgrade soil is considered as 2%. To use the cement-treated soil as subbase and base course, the conventional GSB and base will be replaced with the durable treated soil sample of 25-6-1.0 which satisfies the criteria. The design thickness of the low volume pavement replacing the granular base and subbases with treated soil is tabulated in Table 7, and the cross section of the proposed pavement is depicted in Fig. 10.

Table 8 The design of high volume roads for conventional pavement

Traffic (msa)	Pavement layer thickness (mm)						Strains	
							$\epsilon_z (10^{-4})$	$\epsilon_t (10^{-4})$
	MRB (MPa)	GSB	WMM	Binder course	Surface course			
5	163	150	250	60	30	5.374	3.700	
10	172	200	250	70	40	4.125	4.987	
20	172	200	250	95	40	3.595	2.413	
30	172	200	250	110	40	3.316	2.136	
40	172	200	250	120	40	3.145	1.977	
50	172	200	250	130	40	2.986	1.837	

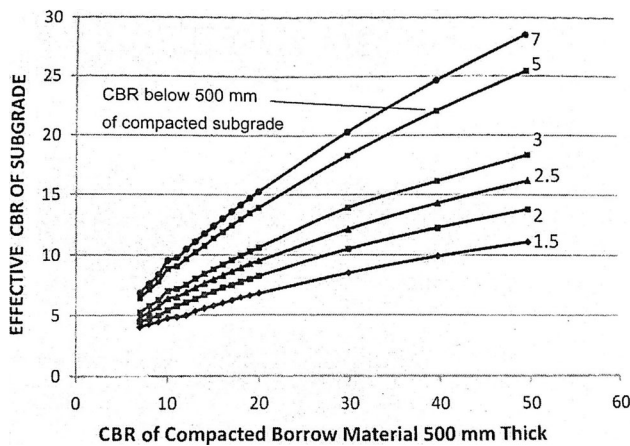


Fig. 11 The effective CBR of the subgrade suggested by IRC: 37-2012

High Volume Roads

The high volume roads are designed using the IRC:37-2018, and the thickness of conventional pavement is tabulated in Table 8. The CBR of the natural subgrade soil is 2%; therefore, the modified soil having CBR more than or equal to 10% should be laid. Hence, effective CBR is found to be 6% from Fig. 11 as per IRC: 37-2012 and the resilient

modulus of the modified subgrade is found to be 55 MPa using the Eq. (2).

$$M_R = 17.6 \times (CBR)^{0.64} \tag{2}$$

The modulus of elasticity of surface course consisting of the binder course and surface course is considered to be 3000 MPa, whereas the elastic modulus of conventional Wet Mix Macadam (WMM), GSB are calculated together using Eq. (3) as suggested by IRC: 37-2018. The horizontal tensile strain (ϵ_t) and vertical compressive strain (ϵ_z) of the conventional pavements are analyzed from the pavement analysis software IITPAVE, and the results are tabulated in Table 8.

$$M_{RB} = 0.2 \times (h)^{0.45} \times M_R \tag{3}$$

To use the stabilized soil as a base course, the CBR of natural soil is 2%, the top 500 mm of the natural soil is excavated and replaced with the modified soil having CBR more than or equal to 10%. The effective CBR of the subgrade soil is found to be 6% from Fig. 11. Hence, the resilient modulus of the modified subgrade soil is calculated using Eq. (2) and is found to be 55 MPa. The GSB should be laid above the modified soil, and the elastic modulus is found to be 120 MPa using Eq. (3). As per IRC:37-2012, the materials to be used as a base course

Table 9 The thickness of the high volume roads using stabilized soil

Traffic (msa)	Thickness (mm)				Strains	
	GSB	Cement-treated base, Stabilized soil 25-6-1.0	Binder course	Surface course	$\epsilon_z (10^{-4})$	$\epsilon_t (10^{-4})$
5	200	155	50	30	5.107	1.933
10	200	165	50	30	4.893	1.895
20	200	185	55	30	4.391	1.808
30	200	170	60	40	4.305	1.742
40	200	175	60	40	4.220	1.727
50	200	175	60	40	4.220	1.727

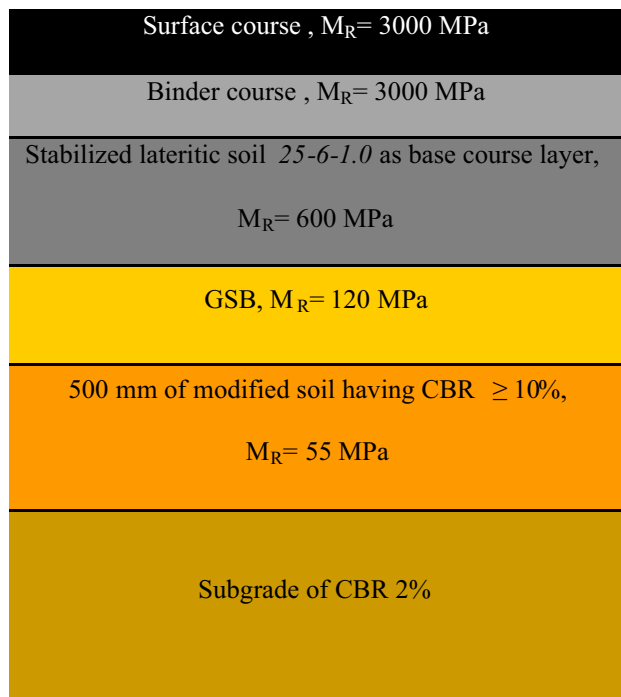


Fig. 12 The cross section of the proposed high-volume road

should have a minimum modulus of 4500 MPa and the modulus of the stabilized soil is calculated using Eq. (4). The resilient modulus of the stabilized soil sample 25-6-1.0 is found to have a UCS of 4615 MPa for heavy compaction. Hence, it can be replaced with a conventional base course.

$$M_R = 1000 \times UCS \quad (4)$$

As the 4615 MPa is too high, the modulus value of 600 MPa is considered for the analysis. The stabilized soil as a base course will be followed by the binder course and surface course together having a modulus of elasticity of 3000 MPa. The strains obtained from the proposed pavement were found less than that of the strains from the conventional pavement. The thicknesses of the proposed high volume roads are tabulated in Table 9. The cross section of the pavement with stabilized soil as a base course is depicted in Fig. 12. When the granular base course is replaced with stabilized soil (cement-treated base), the high strength achieved by the treated soil makes pavement structure semi-rigid. This stabilized soil develops cracks due to shrinkage in due course of time. These cracks will be propagated to the top layer. In order to arrest the propagation of these cracks, an aggregate layer of 100 mm thick is laid as a crack arresting layer as suggested by IRC: 37-2018.

Based on the laboratory test results, the sample of 25-6-1.0 is meeting the requirements of the base course in the pavement construction. Hence, the following conclusions are drawn with respect to the sample of 25-6-1.0.

Conclusions

- The lateritic soil sample treated with 25% GGBFS and alkali solutions consisting of 6% Na₂O and silica modulus of 1.0 has achieved the highest UCS of 5452 and 6593 kPa after 28 days curing for light and heavy compactions, respectively, and found durable under extreme weather conditions.
- The soil sample treated with 25% GGBFS and alkali solutions containing 6% Na₂O and silica modulus of 1.0 has attained the highest flexural strength of 6.3 MPa under heavy compaction and sustained the fatigue life of 5×10^5 .
- The microstructure of the treated sample showed the closely packed and densified structure contributing strength to the mixture.
- The low and high volume road design was suggested replacing the conventional base course with the lateritic soil sample treated 25% GGBFS and alkali solutions containing 6% Na₂O and silica modulus of 1.0.
- A 100 mm of aggregate interface layer should be laid above the base course to avoid propagation of cracks as the strength achieved by the base course is high which makes the pavement rigid.

Compliance with Ethical Standards

Conflict of interest The authors declare that they have no conflict of interest.

References

1. Tremblay H, Leroueil S, Locat J (2001) Mechanical improvement and vertical yield stress prediction of clayey soils from eastern Canada treated with lime or cement. *Can Geotech J* 38:567–579. <https://doi.org/10.1139/t00-119>
2. Qian J, Liang G, Ling J et al (2017) Laboratory characterization of cement-lateritic gravel for use in base construction. *J Mater Civ Eng* 29:1–7. [https://doi.org/10.1061/\(ASCE\)MT.1943-5533.0001466](https://doi.org/10.1061/(ASCE)MT.1943-5533.0001466)
3. Edeh JE, Agbede IO, Tyoyila A (2014) Evaluation of sawdust ash-stabilized lateritic soil as highway pavement material. *J Mater Civ Eng* 26:367–373. [https://doi.org/10.1061/\(ASCE\)MT.1943-5533.0000795](https://doi.org/10.1061/(ASCE)MT.1943-5533.0000795)
4. Paige-Green P, Pinard M, Netterberg F (2015) A review of specifications for lateritic materials for low volume roads. *Transp Geotech* 5:86–98. <https://doi.org/10.1016/j.trgeo.2015.10.002>
5. Adebisi NO, Adeyemi GO, Oluwafemi OS, Songca SP (2013) Important properties of clay content of lateritic soils for engineering project. *J Geogr Geol* 5:99–115. <https://doi.org/10.5539/jgg.v5n2p99>
6. Gidigas M (1976) Laterite soil engineering: pedogenesis and engineering principles. Elsevier, Amsterdam
7. Eluozo SN, Nwaobakata C (2012) Predictive models to determine the behavior of plastic and liquid limit of Lateritic soil for Road construction at Egbema: Imo state of Nigeria. *Int J Eng Technol* 2:25. <https://doi.org/10.14419/ijet.v2i1.425>

8. Mengue E, Mroueh H, Lancelot L, Eko RM (2017) Mechanical improvement of a fine-grained lateritic soil treated with cement for use in road construction. *J Mater Civ Eng* 29:1–22. [https://doi.org/10.1061/\(ASCE\)MT.1943-5533.0002059](https://doi.org/10.1061/(ASCE)MT.1943-5533.0002059)
9. Attoh-Okine NO (1995) Lime treatment of laterite soils and gravels—revisited. *Constr Build Mater* 9:283–287. [https://doi.org/10.1016/0950-0618\(95\)00030-J](https://doi.org/10.1016/0950-0618(95)00030-J)
10. Jawad IT, Taha MR, Majeed ZH, Khan TA (2014) Soil stabilization using lime: advantages, disadvantages and proposing a potential alternative. *Res J Appl Sci Eng Technol* 8:510–520
11. Yoder EJ, Witzczak MW (1991) Principles of pavement design. Wiley, New York
12. Olinic T, Olinic E (2016) The effect of quicklime stabilization on soil properties. *Agric Agric Sci Procedia* 10:444–451. <https://doi.org/10.1016/j.aaspro.2016.09.013>
13. Lekha BM, Goutham S, Shankar AUR (2015) Evaluation of lateritic soil stabilized with Arecanut coir for low volume pavements. *Transp Geotech* 2:20–29. <https://doi.org/10.1016/j.trgeo.2014.09.001>
14. Pooni J, Giustozzi F, Robert D et al (2019) Durability of enzyme stabilized expansive soil in road pavements subjected to moisture degradation. *Transp Geotech* 21:100255. <https://doi.org/10.1016/j.trgeo.2019.100255>
15. Mahvash S, López-Querol S, Bahadori-Jahromi A (2017) Effect of class F fly ash on fine sand compaction through soil stabilization. *Heliyon* 3:e00274. <https://doi.org/10.1016/j.heliyon.2017.e00274>
16. Amu O, Ogunniyi S, Oladeji O (2011) Geotechnical properties of lateritic soil stabilized with sugarcane straw ash. *Am J Sci Ind Res* 2:323–331. <https://doi.org/10.5251/ajsir.2011.2.2.323.331>
17. Alawaji HA (2001) Settlement and bearing capacity of geogrid-reinforced sand over collapsible soil. *Geotext Geomembranes* 19:75–88. [https://doi.org/10.1016/S0266-1144\(01\)00002-4](https://doi.org/10.1016/S0266-1144(01)00002-4)
18. Rajesh S, Viswanadham BVS (2009) Evaluation of geogrid as a reinforcement layer in clay based engineered barriers. *Appl Clay Sci* 46:153–165. <https://doi.org/10.1016/j.clay.2009.07.019>
19. Yang G, Liu H, Lv P, Zhang B (2012) Geogrid-reinforced lime-treated cohesive soil retaining wall: case study and implications. *Geotext Geomembranes* 35:112–118. <https://doi.org/10.1016/j.geotextmem.2012.09.001>
20. Sekhar DC, Nayak S, Preetham HK (2017) Influence of granulated blast furnace slag and cement on the strength properties of lithomargic clay. *Indian Geotech J* 47:384–392. <https://doi.org/10.1007/s40098-017-0228-8>
21. Yadu L, Tripathi RK (2013) Effects of granulated blast furnace slag in the engineering behaviour of stabilized soft soil. *Procedia Eng* 51:125–131. <https://doi.org/10.1016/j.proeng.2013.01.019>
22. Davidovits J (1991) Geopolymers—inorganic polymeric new materials. *J Therm Anal* 37:1633–1656. <https://doi.org/10.1007/BF01912193>
23. Thomas A, Tripathi RK, Yadu LK (2018) A laboratory investigation of soil stabilization using enzyme and alkali-activated ground granulated blast-furnace slag. *Arab J Sci Eng* 43:5193–5202. <https://doi.org/10.1007/s13369-017-3033-x>
24. Stempkowska A, Mastalska-Popławska J, Izak P et al (2017) Stabilization of kaolin clay slurry with sodium silicate of different silicate moduli. *Appl Clay Sci* 146:147–151. <https://doi.org/10.1016/j.clay.2017.05.046>
25. Allahverdi A, Najafi Kani E, Esmaeilpoor S (2008) Effects of silica modulus and alkali concentration on activation of blast-furnace slag. *Iran J Mater Sci Eng* 5:32–35
26. Qureshi MN, Ghosh S (2013) Effect of alkali content on strength and microstructure of GGBFS paste. *Glob J Res Eng Civ Struct Eng* 13:11–20
27. Patankar SV, Jamkar SS, Ghugal YM (2013) Effect of water-to-geopolymer binder ratio on the production of fly ash based geopolymer concrete. *Int J Adv Technol Civ Eng* 2:79–83. <https://doi.org/10.13140/2.1.4792.1284>
28. Cho YK, Yoo SW, Jung SH et al (2017) Effect of Na₂O content, SiO₂/Na₂O molar ratio, and curing conditions on the compressive strength of FA-based geopolymer. *Constr Build Mater* 145:253–260. <https://doi.org/10.1016/j.conbuildmat.2017.04.004>
29. Chi M, Huang R (2012) Effects of dosage and modulus ratio of alkali-activated solution on the properties of slag mortars. *Adv Sci Lett* 16:7–12. <https://doi.org/10.1166/asl.2012.3313>
30. Chi M (2015) Effects of modulus ratio and dosage of alkali-activated solution on the properties and micro-structural characteristics of alkali-activated fly ash mortars. *Constr Build Mater* 99:128–136. <https://doi.org/10.1016/j.conbuildmat.2015.09.029>
31. Petermann JC, Saeed A, Hammons MI (2010) Alkali-activated geopolymers: a literature review. Air Force Research Laboratory Materials and Manufacturing Directorate. Air Force Materiel Command United States Air Force Tyndall Air Force Base, FL, pp 32403–5323
32. Yadollahi MM, Benli A, Demirboğa R (2015) The effects of silica modulus and aging on compressive strength of pumice-based geopolymer composites. *Constr Build Mater* 94:767–774. <https://doi.org/10.1016/j.conbuildmat.2015.07.052>
33. Rios S, Cristelo N, da Fonseca AV, Ferreira C (2016) Structural performance of alkali-activated soil ash versus soil cement. *J Mater Civ Eng* 28:1–30. [https://doi.org/10.1061/\(ASCE\)MT.1943-5533.0001398](https://doi.org/10.1061/(ASCE)MT.1943-5533.0001398)
34. Miao S, Shen Z, Wang X et al (2017) Stabilization of highly expansive black cotton soils by means of geopolymerization. *J Mater Civ Eng* 29:1–9. [https://doi.org/10.1061/\(ASCE\)MT.1943-5533.0002023](https://doi.org/10.1061/(ASCE)MT.1943-5533.0002023)
35. Fasihnikoutalab MH, Asadi A, Unluer C et al (2017) Utilization of alkali-activated olivine in soil stabilization and the effect of carbonation on unconfined compressive strength and microstructure. *J Mater Civ Eng* 29:1–11. [https://doi.org/10.1061/\(ASCE\)MT.1943-5533.0001833](https://doi.org/10.1061/(ASCE)MT.1943-5533.0001833)
36. Pourakbar S, Asadi A, Huat BBK et al (2017) Application of alkali-activated agro-waste reinforced with wollastonite fibers in soil stabilization. *J Mater Civ Eng* 29:1–11. [https://doi.org/10.1061/\(ASCE\)MT.1943-5533.0001735](https://doi.org/10.1061/(ASCE)MT.1943-5533.0001735)
37. Amulya S, Ravi Shankar AU, Praveen M (2018) Stabilisation of lithomargic clay using alkali activated fly ash and ground granulated blast furnace slag. *Int J Pavement Eng*. <https://doi.org/10.1080/10298436.2018.1521520>
38. Phoo-Ngermkham T, Maegawa A, Mishima N et al (2015) Effects of sodium hydroxide and sodium silicate solutions on compressive and shear bond strengths of FA-GBFS geopolymer. *Constr Build Mater* 91:1–8. <https://doi.org/10.1016/j.conbuildmat.2015.05.001>
39. Pnias D, Giannopoulou IP, Perraki T (2007) Effect of synthesis parameters on the mechanical properties of fly ash-based geopolymers. *Colloids Surfaces A Physicochem Eng Asp* 301:246–254. <https://doi.org/10.1016/j.colsurfa.2006.12.064>
40. Memon FA, Nuruddin MF, Khan S et al (2013) Effect of sodium hydroxide concentration on fresh properties and compressive strength of self-compacting geopolymer concrete. *J Eng Sci Technol* 8:44–56
41. Firdous R, Stephan D (2019) Effect of silica modulus on the geopolymerization activity of natural pozzolans. *Constr Build Mater* 219:31–43. <https://doi.org/10.1016/j.conbuildmat.2019.05.161>
42. Dempsey BJ, Thompson MR (1968) Durability properties of lime-soil Mixtures. *Highw Res Board* 235:61–75

Publisher's Note Springer Nature remains neutral with regard to jurisdictional claims in published maps and institutional affiliations.